2182 (1970).
[42]S. Wemple and M. DiDomenico, Jr., Phys. Rev. Letters 23, 1156 (1969).
[43]H. R. Philipp and H. Ehrenreich, Phys. Rev. 129, 1550 (1963); 131, 2016 (1963); 131, 2016 (1963).
[44]M. Cardona and D. L. Greenaway, Phys. Rev. 133, A1685 (1964).
[45]T. M. Donovan, E. J. Ashley, and H. E. Bennett, J. Opt. Soc. Ann. 53, 12 (1963); 53, 1403 (1963).
[46]H. E. Bennett and J. O. Porteus, J. Opt. Soc. Am. 51, 123 (1961).
[47]D. R. Huffman (private communication).
[48]D. M. Roessler, Brit. J. Appl. Phys. 16, 1119 (1965).
[49]I. Drabkin, L. Emel'yanova, R. Iskenderov, and Ya. Ksendzov, Fiz. Tverd. Tela 10, 3082 (1968) [Sov. Phys. Solid State 10, 2428 (1969)].
[50]Photoconductivity measurements performed by E. R. Middlemiss, University of California, Riverside, Calif.
[51]W. E. Spicer, Phys. Rev. 154, 385 (1967).
[52]D. Adler, IBM J. Res. Develop. 14, 261 (1970).
[53]L. Marton, Rev. Mod. Phys. 28, 172 (1956).
[54]D. Pines, *Elementary Excitations in Solids* (Benjamin, New York, 1963).
[55]S. L. Adler, Phys. Rev. 126, 413 (1962).
[56]H. Ehrenreich and H. R. Philipp, *Proceedings of the International Conference on the Physics of Semiconductors, Exeter* (The Institute of Physics and Physical Society, London, 1962).
[57]C. B. Wilson, Proc. Phys. Soc. (London) 76, 481 (1960).
[58]H. Ehrenreich and H. R. Philipp, Phys. Rev. 128, 1622 (1962).
[59]J. L. McNatt, Phys. Rev. Letters 23, 915 (1969).

PHYSICAL REVIEW B VOLUME 4, NUMBER 10 15 NOVEMBER 1971

Third-Harmonic Generation in Absorbing Media of Cubic or Isotropic Symmetry*

W. K. Burns† and N. Bloembergen
Division of Engineering and Applied Physics, Harvard University, Cambridge, Massachusetts 02138
(Received 14 May 1971)

Third-harmonic generation in strongly absorbing media has been measured in reflection, by means of a picosecond pulse train from a mode-locked Nd-glass laser. The nonlinear susceptibility $\chi^{(3)}(3\omega)$ has been measured in the semiconductors diamond, Si, Ge, and GaAs, and the metals Be, Mg, Al, Cu, Ag, and Au relative to LiF. The data are compared with data for $\chi^{(3)}$ obtained in the infrared from frequency mixing with CO_2 lasers. The different dispersion characteristics for valence- and conduction-band contributions are pointed out. The cubic anisotropy of $\chi^{(3)}(3\omega)$ in silicon and several alkali halide crystals is determined by means of circularly polarized laser pulses. The selection rules for the generation of circularly polarized third harmonics have been confirmed both in transparent and in absorbing media.

I. INTRODUCTION

Optical third-harmonic generation (THG) in transmission was first detected by phase matching in calcite by Terhune *et al.*[1] They also measured the susceptibility and anisotropy in LiF and other alkali halide crystals.[2] THG in gases was observed by New and Ward.[3] They discovered that phase-cancellation effects from focusing into a homogeneous medium of infinite extent eliminate THG. Phase-matched THG was achieved in a liquid by Bey *et al.*[4] by utilizing the anomalous dispersion due to dye molecules placed in a normally dispersive liquid. The same workers also observed THG in reflection from the same dye-liquid combination by achieving phase matching near the critical angle for total internal reflection.[5] Non-phase-matched THG in reflection was observed by Wang and Baardsen,[6] who remeasured TH susceptibilities for the alkali halides and glass. The first reflected THG from strongly absorbing media was reported by Bloembergen *et al.*[7]

The observed signals are necessarily weak, since they are generated by a higher-order nonlinear polarization in the small absorption depth at the third-harmonic frequency. The intensity of the incident laser light must be high, and yet thermal damage due to absorption cannot be tolerated. If the medium is also strongly absorbing at the fundamental, the use of high-intensity picosecond laser pulses is essential. In this paper more details on the experimental method and more complete experimental data are presented. The dispersion of the nonlinear susceptibility in the absorbing frequency ranges is of theoretical interest.

In Sec. II the pertinent theory of THG in reflection and transmission is briefly reviewed. Section III describes the experimental techniques. In Sec. IV we present the experimental results for some semiconductor crystals of cubic symmetry, including diamond, Si, Ge, and GaAs. The dispersive behavior of $\chi^{(3)}$ is discussed and a comparison with other data for $\chi^{(3)}$ obtained from frequency mixing in the infrared is made. The influence of conduction electrons and surface preparation is investigated. In Sec. V the cubic anisotropy of $\chi^{(3)}$ in

alkali halide crystals and semiconductors is determined, and experimental results for THG by circularly polarized laser beams in absorbing media are described. It is established that the selection rules for the generation of circularly polarized harmonics[8-11] are also valid in absorbing media. This is of interest and relates to the question of conservation of angular momentum in the generation of circularly polarized harmonics.[12,13] It is shown how the theory can be extended to include dissipative processes.

In Sec. VI the results for THG in some polycrystalline metals, Be, Mg, Al, Cu, Ag, and Au are given. The dependence of THG on the angle of incidence is determined and the variation of $\chi^{(3)}$ in different metals is discussed.

II. REVIEW OF THG THEORY

A theoretical expression for the TH polarization in a nonlinear medium was first given by Armstrong *et al.*,[14] and the waves created by this polarization, both in reflection and transmission, were discussed by Bloembergen and Pershan.[15] Much work has been done on reflected second-harmonic generation.[16] The theory for THG is entirely analogous and the purpose of this section is merely to present the equations necessary to derive the nonlinear susceptibility tensor $\chi^{(3)}$ from the experimental observations.

The symmetry properties of $\chi^{(3)}$ for THG have been given by Terhune *et al.*[1] In cubic crystals of point group symmetry 432, $\bar{4}3m$ or $m3m$ the tensor has only two independent elements and the nonlinear TH polarization has components given by

$$P_i^{\mathrm{NL}}(3\omega) = 3\chi^{(3)}_{xxyy} E_i(\vec{E}\cdot\vec{E}) + (\chi^{(3)}_{xxxx} - 3\chi^{(3)}_{xxyy})E_i^3, \quad (1)$$

where i refers to the three cubic axes $\hat{x}$, $\hat{y}$, and $\hat{z}$. For isotropic materials, the TH polarization is always parallel to the applied fundamental field, and $\chi^{(3)}_{xxxx} = 3\chi^{(3)}_{xxyy}$ is the isotropy condition.

A useful experimental geometry is one in which both the laser and the third-harmonic electric fields are polarized normal to the plane of incidence. This may be achieved in several ways in a crystal, whose face normal is in the [001] direction. The laser may be polarized along the [010] direction, or by rotating the crystal around its normal by 45°, along a $[1\bar{1}0]$ direction. In the first case the nonlinear polarization perpendicular to the plane of incidence has the magnitude

$$P_\perp^{\mathrm{NL}}(3\omega) = \chi^{(3)}_{xxxx}(E_\perp)^3 , \quad (2)$$

and in the second case

$$P_\perp^{\mathrm{NL}}(3\omega) = \tfrac{1}{2}(\chi^{(3)}_{xxxx} + 3\chi^{(3)}_{xxyy})(E_\perp)^3 . \quad (3)$$

Here $E_\perp$ is the laser field inside the medium and is related to the incident laser amplitude by the Fresnel formula

$$E_\perp = E_\perp^{(i)} \frac{2\cos\theta_i}{\cos\theta_i + \epsilon_1^{1/2}(1-\sin^2\theta_i)^{1/2}} . \quad (4)$$

Here θ_i is the angle of incidence and $\epsilon_1^{1/2}$ is the index of refraction at the laser frequency. The amplitude of the reflected TH wave is proportional to $P_\perp^{\mathrm{NL}}(3\omega)$ and the observed reflected harmonic intensity is determined by

$$|E_{3\perp}^R|^2 = |\chi|^2 F_\perp^R(\theta_i, \epsilon)\,|E_\perp^i|^6 . \quad (5)$$

Here χ stands for the relevant combination of tensor elements in Eqs. (2) and (3), respectively, and $F_\perp^R$ is a function of the angle of incidence and the indices of refraction, $\epsilon_1^{1/2}$ at ω and $\epsilon_3^{1/2}$ at 3ω, which are complex quantities in an absorbing medium;

$$F_\perp^R(\theta_i, \epsilon) = \frac{1024\pi^2\cos^6\theta_i}{|\cos\theta_i + (\epsilon_1 - \sin^2\theta_1)^{1/2}|^6\,|\cos\theta_i + (\epsilon_3 - \sin^2\theta_i)^{1/2}|^2} \frac{1}{|(\epsilon_1 - \sin^2\theta_i)^{1/2} + (\epsilon_3 - \sin^2\theta_i)^{1/2}|^2} . \quad (6)$$

If the nonlinear medium is transparent at the fundamental frequency, the THG can also be observed in transmission. It will be assumed that multiple reflections of the fundamental beam may be ignored. This will be the case if the Fresnel reflection coefficient is small (it enters THG formulas with a high power), or if multiple reflections do not overlap in space because the angle of the light beam with the normal is sufficiently large. In general, the TH field in the medium, consists of a driven inhomogeneous solution of the wave equation with wave vector $\vec{k}_3^S = 3\vec{k}_1^T$ equal to three times the wave vector of the transmitted laser beam, and a homogeneous solution of the wave equation with wave vector $\vec{k}_3^T$. The field observed just outside the slab of thickness r is

$$E_{3\perp}^T = \frac{4\pi P_\perp^{\mathrm{NL}}}{\epsilon_1 - \epsilon_3}\left(f_S e^{i\vec{k}_3^S\cdot\vec{r}} - f_T e^{i\vec{k}_3^T\cdot\vec{r}}\right) , \quad (7)$$

where we have kept account of the fact that the Fresnel factors for transmission at the exit plane are, in principle, slightly different. We have

$$f_S = \frac{(\epsilon_1 - \sin^2\theta_i)^{1/2} + (\epsilon_3 - \sin^2\theta_i)^{1/2}}{(\epsilon_3 - \sin^2\theta_i)^{1/2} + \cos\theta_i} , \quad (8)$$

$$f_T = \frac{2(\epsilon_3 - \sin^2\theta_i)^{1/2}}{(\epsilon_3 - \sin^2\theta_i)^{1/2} + \cos\theta_i} . \quad (9)$$

The observed TH transmitted intensity is proportional to $|E_{3\perp}^T|^2$. If the medium is absorbing at 3ω,

$\vec{k}_3^T$ is complex and the homogeneous wave solution has decayed exponentially close to zero at the exit face. In this case the TH transmitted intensity is independent of the sample thickness. If the medium is transparent at both ω and 3ω, and if the difference in Fresnel factors is ignored ($f_S \approx f_T$), one finds the equation, which exhibits the familiar oscillatory character due to the finite coherence length,

$$|E_{3l}^T|^2 = \frac{64\pi^2|\chi|^2}{(\epsilon_1-\epsilon_3)^2}\,|E_1^i|^6\left(\frac{2\cos\theta_i}{\cos\theta_i+(\epsilon_1-\sin^2\theta_i)^{1/2}}\right)^6 \frac{4(\epsilon_3-\sin^2\theta_i)}{[(\epsilon_3-\sin^2\theta_i)^{1/2}+\cos\theta_i]^2}\sin^2\frac{\pi z}{l_{\rm coh}(\theta_i)}\ , \tag{10}$$

with $l_{\rm coh}$ determined by

$$\tfrac{1}{2}(3\omega/c)[(\epsilon_1-\sin^2\theta_i)^{1/2}-(\epsilon_3-\sin^2\theta_i)^{1/2}]l_{\rm coh}=\pi\ . \tag{11}$$

If the difference between f_S and f_T is taken into account, there would not be precise nulls in the transmitted intensity; Eq. (10) is an approximation.

The equations for the case, when the nonlinear polarization has a component in the plane of incidence, are generally more complicated. For isotropic substances the fields at the fundamental and TH frequency are parallel to each other. If they both lie in the plane of incidence, the following expression replaces Eq. (6) for the reflection case:

$$F_{\parallel}^R(\theta_i,\epsilon)=1024\pi^2\left|\frac{\epsilon_1}{\epsilon_1-\epsilon_3}\right|^2 \frac{\cos^6\theta_i\,|\,\epsilon_3(\epsilon_1-\sin^2\theta_i)^{1/2}-\epsilon_1(\epsilon_3-\sin^2\theta_i)^{1/2}|^2}{|\,(\epsilon_1-\sin^2\theta_i)^{1/2}+\epsilon_1\cos\theta_i|^6\,|\,\epsilon_3\cos\theta_i-\epsilon_1(\epsilon_3-\sin^2\theta_i)^{1/2}|^2}\ . \tag{6'}$$

The components of the susceptibility tensor can be determined exclusively from measurements with the harmonic polarization normal to the plane of incidence. In absorbing media the components of $\chi^{(3)}$ are complex. From the intensity measurements only absolute values such as $|\chi^{(3)}_{xxxx}|$ and $|\chi^{(3)}_{xxxx}+3\chi^{(3)}_{xxyy}|$, or other linear combinations may be obtained. The phase factors of the complex susceptibility tensor elements can, in principle, be determined unambiguously by an interference experiment, where the same laser beam produces TH in a transparent medium with real $\chi^{(3)}$ and in the absorbing medium.[16]

It should be emphasized that the real and imaginary parts both transform in the same manner under the operations of the crystallographic point group. The symmetry conditions imposed by cubic symmetry, or isotropy, remain valid for the complex tensor elements. The permutation symmetry condition, which holds for the real part, is, however, generally not valid for the imaginary part. This is equivalent to saying that the Onsager symmetry relation, valid for linear dissipative processes, does not generally exist in the nonlinear case.[13]

It is of interest to consider especially the case of circular polarization for light waves incident normally on the nonlinear medium. For a circularly polarized amplitude one has $\vec{E}\cdot\vec{E}=0$. Equation (1) shows that the TH polarization then vanishes in isotropic media. It also shows that for a circularly polarized light wave propagation along a cubic axis, e.g., in the $\hat{z}$ [001] direction, $\vec{E}=A(\hat{x}\pm i\hat{y})$, the TH polarization is circularly polarized in the opposite sense

$$\vec{P}_i^{\rm NL}(3\omega)=(\chi_{xxxx}-3\chi_{xxyy})A^3(\hat{x}\mp i\hat{y})\ . \tag{12}$$

This equation shows that the circularly polarized TH is a direct measure of the cubic anisotropy of $\chi^{(3)}$. Group-theoretical arguments or explicit calculations with the Cartesian tensor elements of $\chi^{(3)}$ can also show that a circularly polarized laser beam propagating along an axis of fourfold symmetry in any material, must always produce a TH polarization circulating in the opposite sense, and that a circularly polarized laser beam propagating along a threefold or sixfold axis of symmetry cannot produce any TH polarization.[10,11] Since these are properties based on crystal symmetry, they hold equally in transparent and in absorbing media. For the present investigations the important implication is that a circularly polarized laser beam propagating along the body diagonal [111] in a cubic crystal or in an isotropic absorbing medium cannot produce TH generation.

III. EXPERIMENTAL TECHNIQUES

A. Apparatus

The laser used in these experiments was a Nd^{+3}-glass mode-locked laser similar to that described by DeMaria *et al.*[17] This type of laser was an essential part of the experiment because its unique time structure of ultrashort pulses combines the characteristics of high intensity with low energy. These properties are precisely what is needed to observe THG in strongly absorbing media. High intensity is required to generate TH while low energy is necessary to avoid surface damage and thermal radiation.

The optical length of the cavity was 1.25 m, and the front and back mirrors were 35 and 99.9% re-

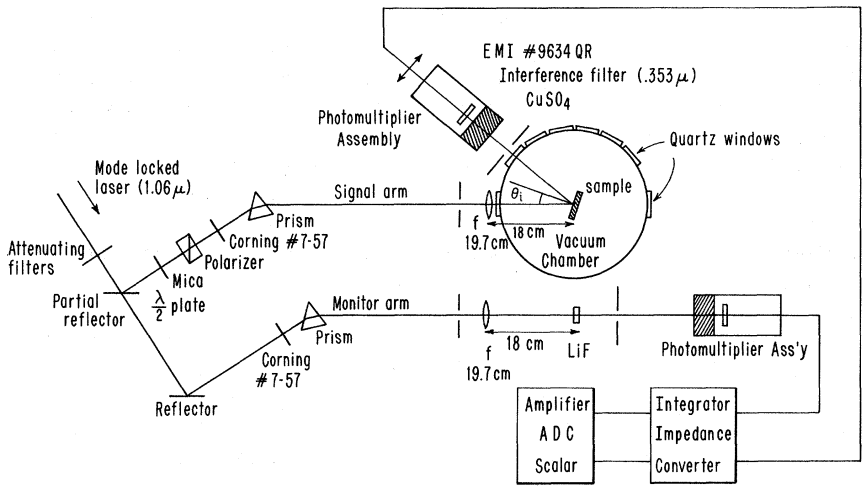

FIG. 1. Schematic of the experimental arrangement to measure THG in reflection and transmission.

flecting, respectively. The laser rod was a silicate-glass double-Brewster-angle rod with 3% neodymium doping made by Owens-Illinois. Its dimensions were 7 in. long and $\frac{3}{8}$ in. in diameter. The laser was passively mode locked by Eastman 9860 Q-switch solution at a concentration of 1.5% by volume in 1,2-dichloroethane. This gave a small signal transmission of 87% in a dye cell 3 mm thick. The rod was pumped in a dual elliptical water-cooled cavity. Due to efficient cooling and low-energy input (375 J per flash), the laser could be fired every 20 sec.

The mode-locked pulse trains varied in length from 150 to 600 nsec. The energy output was 0.2–0.4 J with a power density of $(2-5)\times10^9$ W/cm^2. The mode-locked pulse duration was measured by the two-photon fluorescence technique to be approximately 4.5 psec. The beam divergence was measured to be about 0.2 mrad.

The experimental arrangement used in most of these experiments is shown in Fig. 1. The laser beam is divided into two parts, each of which traverses a separate measuring arm of the experiment. The sample of interest is placed in the signal arm, for measurement in reflection or transmission. In the monitor arm, TH is generated in a fixed LiF crystal in transmission. This monitor signal calibrates the laser intensity for each firing of the laser.

Since THG does not require a lack of inversion symmetry, it can be generated both in glass and in air. It was found that a large amount of TH was generated in the laser itself, probably from the glass rod. Filters such as Corning No. 7-57, which absorb blue light, generate TH in the last absorption depth near the exit face. These filters also tend to emit broad-band fluorescence when irradiated by high-intensity laser radiation. For these reasons a prism was used in each arm to separate the fundamental at 1.06 μm from any blue light that may be present. In order to eliminate TH generated in the air, the laser was focused behind the sample in a vacuum chamber. The TH generated from the lens, windows, and the air outside the chamber was small compared to the signal, because the beam intensity is much higher at the sample. It has been shown that through an ideal focus, there should be exact phase cancellation of THG in air.[3] Here the partially reflecting sample is just before the focal region and this phase cancellation is not exact. One then observes the interference of the TH generated in the air and in the sample. This was observed with the reflected signal from Ge which increased by a factor of 2 when the atmosphere was admitted to the vacuum chamber. A vacuum of less than 10^{-4} Torr was used to eliminate this problem. It was not necessary to put the monitor crystal in vacuum, since it was only a monitor of laser intensity and it did not matter where the TH was generated.

The vacuum box was constructed with quartz windows every 20° so that reflecting samples could be studied under varying angles of incidence (θ_i) and transparent samples could be studied in transmission. The samples were mounted on a rotating stage which could be adjusted from outside the chamber. Because of Brewster angle faces, the laser beam was predominantly polarized with the E field in the horizontal direction. A Glan-Kappa polarizer defined the state of polarization precisely. When vertical polarization, corresponding to the E field normal to the (horizontal) plane of incidence, was desired, a mica $\lambda/2$ plate was inserted and the Glan-Kappa polarizer turned by 90°.

A major experimental problem was to adjust the laser energy distribution at the sample face so that observable TH was generated without damage to the sample surface. This was particularly im-

portant for Ge and Al which are the most absorbing at 1.06 μm and seemed to damage the most easily. The energy distribution was adjusted by using attenuating filters before the prism and by changing the beam diameter at the sample surface, by varying the position of the lens in front of the chamber window. With a 19.7-cm focal length lens and a ~0.2 mrad diverging beam, the focus was varied from 1–4 cm behind the sample surface. For the easily damaged samples, additional beam expansion was required and a simple telescope with a magnification of two was used before the prism. With the telescope in place, the beam diameter at the sample could be varied from 1 to 3 mm. The intensity at the surface was estimated to be 0.25–1.0 GW/cm^2 depending on the attenuation used for a particular sample. The energy reaching the sample during one entire pulse train was only 2.5 to 10 mJ.

The TH at 0.353 μm was detected by EMI photomultipliers No. 9634 QR. The fundamental at 1.06 μm is absorbed in a saturated solution of $CuSO_4$ in water. Final discrimination is provided by a sharp interference filter (100-Å half-power bandwidth) at 0.353 μm. The filtering was sufficiently selective that no signal was observed when the laser was fired directly into the tube, yet the combination allowed roughly 10% transmission of the TH.

The photomultiplier tubes have an 8-nsec risetime and could not resolve the individual pulses in the mode-locked train. Since the signal amplitude was low, the signal was electronically integrated over the pulse train and the total TH output was observed. The integrated signal was then amplified and measured by an analog-to-digital converter and counting apparatus. This apparatus was dual so that signals from both arms of the experiment were simultaneously counted and displayed.

B. Measurement of $\chi^{(3)}$

Denote the signal and monitor counts by S and M, respectively, and let $\sum$ denote integration over time. One obtains from Eqs. (5)–(11),

$$S = C_S |\chi(\phi)|^2 F(\theta_i, \epsilon) \sum |E_1^i|^6 ,$$
$$M = C_M \sum |E_1^i|^6 , \tag{13}$$

where ϕ specifies the orientation of the sample and where C_S and C_M are experimental proportionality constants for each arm. For the monitor arm $\chi(\phi)$ and $F(\theta_i, \epsilon)$ are absorbed in C_M since they never change and we are only interested in the field dependence. The ratio of the two channel counts is

$$(S/M) = (C_S/C_M) |\chi(\phi)|^2 F(\theta_i, \epsilon) . \tag{14}$$

This explains why it is useful to monitor the fundamental field with the LiF crystal. The laser intensity typically varied by a factor of 2–3 from shot to shot, leading to large variations in the TH output. Even using this technique, the ratio S/M varied somewhat from shot to shot. This was thought to be due to the uncontrolled transverse mode structure in the laser, and variations in amplification in the high-gain ($\times 10^6$) photomultipliers. In practice this problem was overcome by taking 20–30 laser shots and obtaining an average for S/M. This average value was found to be quite reproducible.

All measurements made in this work are relative measurements. After measuring S/M for one sample, it was removed and another sample inserted and measured. The samples were placed so that the generating face of each sample intercepted the focusing beam at the same point. Between the measurements all experimental variables such as filters, amplifier gains, etc., were left unchanged so that C_S and C_M were held constant. The ratio S/M was then measured for the second sample and from Eq. (14) one obtains

$$\frac{(S/M)_1}{(S/M)_2} = \frac{|\chi(\phi)|_1^2}{|\chi(\phi)|_2^2} \frac{F_1(\theta, \epsilon)}{F_2(\theta, \epsilon)} , \tag{15}$$

where the two situations are denoted by 1 and 2. Since the $F(\theta, \epsilon)$ factors are known, from Eqs. (5)–(11), the ratio of the susceptibilities can be measured. This procedure can be used for two reflecting samples, two transmitting samples, or one reflecting and one transmitting sample.

The procedure can also be used to measure the cubic anisotropy of $\chi^{(3)}$, which is defined as the ratio $3\chi^{(3)}_{xxyy}/\chi^{(3)}_{xxxx}$. In this case a sample is cut with the normal along the [001] axis. The signal is measured with the electric field parallel to the [010] axis. Then the sample is turned by 45° around its own normal so that the electric field is parallel to [1$\bar{1}$0]. From Eqs. (15), (2), and (3) the cubic anisotropy may be determined from

$$\frac{(S/M)_{[110]}}{(S/M)_{[010]}} = \frac{1}{4} \left| 1 + \frac{3\chi^{(3)}_{xxyy}}{\chi^{(3)}_{xxxx}} \right|^2 . \tag{16}$$

The anisotropy ratio may be determined with even higher precision by comparing the TH signals produced by a circularly and a linearly polarized laser beam, respectively, propagating along a cubic axis. To this end a polarizer and a $\lambda/4$ plate are inserted between the prism and the lens in the signal arm. The $\lambda/4$ plate can be rotated so as to yield either linear or circular polarization. The light beam is incident normally on the sample along the [001] direction. The linear polarization is parallel to the [100] direction. The ratio of the mean values in these two geometries is given by

$$\frac{(S/M)_{\text{circular}}}{(S/M)_{\text{linear}}} = \frac{1}{4}\left|1 - \frac{3\chi^{(3)}_{xxyy}}{\chi^{(3)}_{xxxx}}\right|^2 + 4\delta^2\left|\frac{3\chi^{(3)}_{xxyy}}{\chi^{(3)}_{xxxx}}\right|^2 . \tag{17}$$

Here the last term on the right-hand side is a small correction term to take account of the fact that exact circular polarization is difficult to achieve.

The quality of the circularly polarized light can be determined by measuring the transmitted TH intensity with circularly and linearly polarized fundamental fields in an isotropic material. By Eq. (17) the ratio of these intensities is $4\delta^2$, which is zero only in the ideal case of perfect circular polarization. It is expected that δ will be nonzero due to the following factors: (i) strain birefringence in the vacuum chamber window; (ii) the divergence of the laser beam passing through the uncompensated $\lambda/4$ plate; (iii) the error in angular orientation of the $\lambda/4$ plate. In practice an axis of the plate was found by inserting the plate between crossed polarizers and rotating the plate until the minimum transmission of a HeNe laser beam was unchanged. An axis of the plate was then parallel to the direction of polarization of the field between the polarizers. When rotated by 45° the plate should produce circular polarization for the glass laser. It was estimated that the plate could be set to within 0.01 rad.

C. Linear Optical Constants

For the evaluation of the nonlinear susceptibilities from Eq. (15) and the functions $F(\theta_i, \epsilon)$ in Eqs. (6), (6′), and (10), it is necessary to know the linear optical constants of the materials used. The complex dielectric constant is related to the tabulated values for the index of refraction n and extinction coefficient κ by $\epsilon = \epsilon' + i\epsilon'' = (n + i\kappa)^2$. The values of n and κ at the fundamental and TH wavelength are given in Table I. The sources are given in the references. The quoted uncertainties lead to considerable variation in $F(\theta_i, \epsilon)$ since the dielectric constant enters with high powers.

The reader is reminded that each material has its own characteristic dispersive behavior of n and κ and that the Fresnel factors may show drastically different behavior as a function of frequency. One particular example, the case of Al, is displayed for future reference in Fig. 2. For other materials the references in Table I may be used.

The angular dependence of the Fresnel functions for TH reflection given by Eqs. (6) and (6′) are displayed for the three materials Si, Al, and Ag in Figs. 3–5. The data must be used to evaluate the nonlinear susceptibilities from Eqs. (15)–(17).

D. Sample Description and Preparation

The metals were measured using polished solid samples and, when possible, evaporated films. The evaporated films gave the best results since it was difficult to keep the polishing agent from contaminating the solid samples. The evaporated films were made on glass slides. The initial

TABLE I. Values of n and κ at the fundamental and TH wavelengths.

	n_1	κ_1	n_3	κ_3
Si[a]	3.55 ±0.18	$(1.1 \pm 0.1) \times 10^{-4}$	$5.55^{+0.55}_{-0.28}$	3.04±0.15
Ge[b,c]	4.36 ±0.22	0.08±0.02	4.08 ±0.20	2.55±0.13
GaAs[d]	3.44 ±0.17	0.02±0.002	3.43 ±0.17	1.92±0.10
Be[e,c]	2.50 ±0.25	3.15±0.19	2.37 ±0.24	2.14±0.21
Mg[f,c]	0.884±0.09	6.45±0.65	0.52 ±0.05	1.55±0.16
Al[g,c] (evap.)	1.44 ±0.07	9.9 ±0.4	0.33 ±0.01	3.93 ±0.3
Cu[c] (evap.)	0.197±0.02	6.65±0.3	0.825±0.03	1.4 ±0.25
Ag[h,c,i] (evap.)	0.134±0.015	7.35±0.10	0.152±0.013	1.30 ± 0.07
Au[j,c,i] (evap.)	0.188±0.012	6.38±0.34	1.45 ±0.07	1.72±0.09
Diamond[k]	2.3914		2.4896	
LiF[c]	1.3868		1.4020	

[a] H. R. Philipp and E. A. Taft, Phys. Rev. 120, 37 (1960); W. C. Dash and R. Newman, *ibid.* 99, 1151 (1955); G. G. McFarlane and V. Roberts, *ibid.* 98, 1865 (1955).
[b] H. R. Philipp and E. A. Taft, Phys. Rev. 113, 1002 (1959).
[c] *American Institute of Physics Handbook*, 2nd ed. (McGraw-Hill, New York, 1963), Sec. 6-g.
[d] H. R. Philipp and H. Ehrenreich, Phys. Rev. 129, 1550 (1963).
[e] I. N. Shklyarevskii and R. G. Yarovaya, Opt. i Spektroskopiya 11, 661 (1961) [Opt. Spectry. (USSR) 11, 355 (1961)].
[f] D. Jones and A. H. Lettington, Proc. Phys. Soc. (London) 92, 948 (1967).
[g] H. Ehrenreich, H. R. Philipp, and B. Segall, Phys. Rev. 132, 1918 (1963); H. Ehrenreich (private communication).
[h] R. S. Minor, Ann. Physik 10, 58 (1903); R. H. Huebner *et al.*, J. Opt. Soc. Am. 54, 1434 (1964).
[i] R. Kretzmann, Ann. Physik 37, 303 (1940).
[j] W. Meier, Ann. Physik 31, 1017 (1910).
[k] F. Peter, Z. Physik 15, 358 (1923).

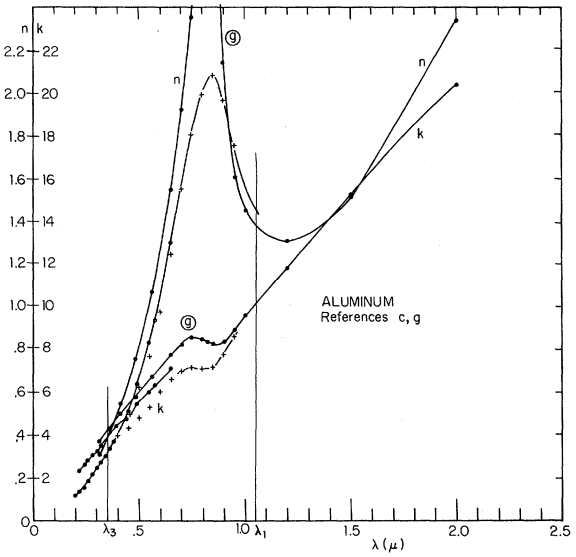

FIG. 2. The complex index of refraction as a function of wavelength in Al (from Refs. c and g of Table I).

polishing step for each material was 1000 mesh SiC on a glass lap wet with ethylene glycol. The details for each metal are given below.

Beryllium: 99% pure nuclear grade Be, purchased from Barden-Leemath and polished by them to a "mirror finish." The surface was protected from the atmosphere by an inert plastic film which was peeled off before the measurement was made.

Magnesium: Cut from rod stock and polished with 0.3-μ alumina (Al_2O_3).

Aluminum: High-purity (99.9999%) single crystal polished with 0.3-μ alumina. The Al evaporated films were made from 99.8% pure wire in the relatively high vacuum of $(4-5)\times10^{-7}$ Torr. A high vacuum is desirable with Al in order to attain a high reflectivity in ultraviolet.[18]

Copper: Cut from high-purity (99.999%) rod and polished with red rouge on Politex Supreme lap.

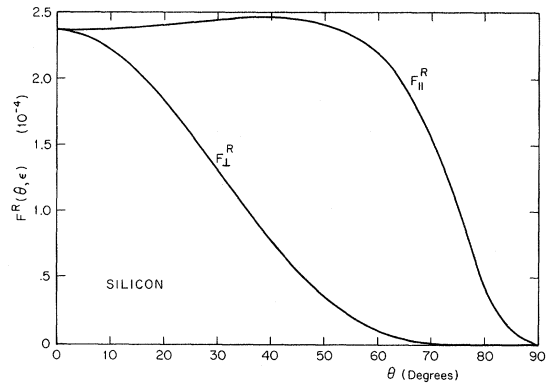

FIG. 3. The Fresnel factors [Eqs. (6) and (6′)] for reflected THG from silicon.

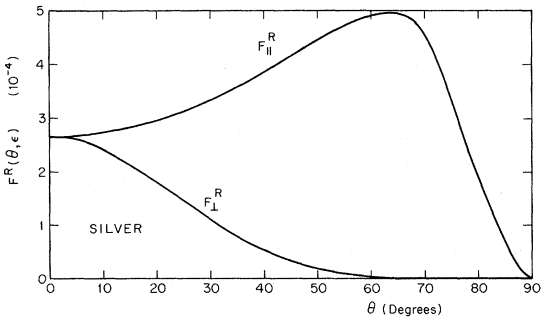

FIG. 4. The Fresnel factors [Eqs. (6) and (6′)] for reflected THG in silver.

The films were made by evaporation from oxygen-free high-conductivity grade wire at $\sim5\times10^{-5}$ Torr vacuum.

Silver: Cut from high-purity (99.999%) rod and polished with red rouge on Politex Supreme lap. The films were made by evaporation from 99.99% pure wire at $\sim5\times10^{-5}$ Torr vacuum.

Gold: Piece of unknown purity polished with 0.3-μ alumina powder. The films were made by evaporation from 99.99% pure wire at $\sim5\times10^{-5}$ Torr vacuum.

The semiconductors were measured after being mechanically polished and after being polished and etched. Again, the first polishing step was 1000

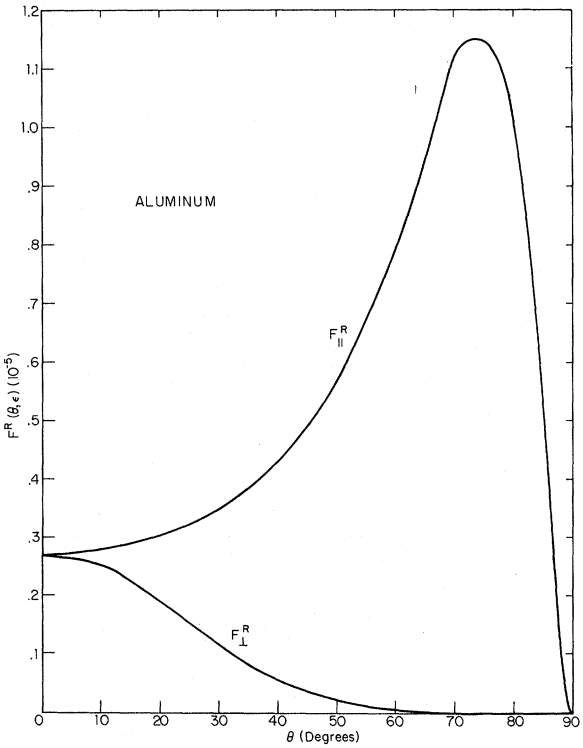

FIG. 5. The Fresnel factors [Eqs. (6) and (6′)] for reflected THG in aluminum.

TABLE II. TH susceptibility of high-resistivity semiconductors relative to LiF.

Material	Quantity observed	Value relative to $\lvert\chi^{(3)}_{xxxx}\rvert$ LiF
Diamond TH transmission	$\frac{1}{2}\lvert\chi^{(3)}_{xxxx}+3\chi^{(3)}_{xxyy}\rvert$	$52\pm10\%$
Silicon polished, TH reflection	$\lvert\chi^{(3)}_{xxxx}\rvert$	$(6.0\times10^{4})\pm30\%$
Silicon polished, TH transmission	$\lvert\chi^{(3)}_{xxxx}\rvert$	$(8.4\times10^{4})\pm50\%$
Germanium polished, TH reflection	$\lvert\chi^{(3)}_{xxxx}\rvert$	$(1.7\times10^{4})\pm50\%$
Germanium etched, TH reflection	$\lvert\chi^{(3)}_{xxxx}\rvert$	$(3.1\times10^{4})\pm80\%$
GaAs etched, TH reflection	$\lvert\chi^{(3)}_{xxxx}\rvert$	$(4.5\times10^{4})\pm50\%$

grit SiC on a glass lap with ethylene glycol. The etches listed are of the chemical polish type. Only mild etching could be tolerated, otherwise the reflections become too diffuse to observe. A short time in a relatively strong etch gave the best results. After etching, the etchant was diluted and displaced with methanol to try to keep surface films from forming.[19] They appeared anyway, particularly on Si and Ge.

Silicon: The undoped material had a resistivity of $\sim 100\,\Omega$ cm at 300° K corresponding to a carrier concentration of $n\sim 5\times10^{13}/\mathrm{cm}^{-3}$. The Si was polished with 1-μ diamond paste followed by $\frac{1}{4}$-μ diamond paste on rotating pelon cloth. Two etches were tried, CP-8 consisting of 5 parts HNO_3 and 3 parts HF, and CP-4A, consisting of 5 parts HNO_3, 3 parts HF and 3 parts CH_3 COOH.

Germanium: The undoped material was intrinsic Ge ($\rho>40\,\Omega$cm, $n\sim10^{13}/\mathrm{cm}^{-3}$). The Ge was polished with 0.3- and in some cases 0.1-μ alumina powder on a wax lap. The etch used was CP-4, consisting of 2 parts HNO_3, 1 part HF, and 1 part CH_3 COOH.

Gallium arsenide: The high-resistivity material was oxygen doped ($\rho\sim2\times10^{5}\,\Omega$ cm, $n<10^{10}/\mathrm{cm}^{-3}$). The GaAs was polished with 0.3-μ alumina powder and was etched for 2 sec in a mixture of 1 part HF, 3 parts HNO_3, and 2 parts H_2O.

The diamond sample used was clear optical quality diamond, 0.9 mm thick, with polished faces about 7° from (111) planes.

The alkali halide samples were plates with the normal in the [001] direction. The samples, obtained from the Harshaw Company were optically polished on both sides, with a thickness between 0.5 and 2 mm.

IV. TH SUSCEPTIBILITY IN SEMICONDUCTORS

In this section results for $\lvert\chi^{(3)}_{xxxx}\rvert$ in Si, Ge, and GaAs will be presented, and for $\frac{1}{2}\lvert\chi^{(3)}_{xxxx}+3\chi^{(3)}_{xxyy}\rvert$ in diamond. The value of $\frac{1}{2}\lvert\chi^{(3)}_{xxxx}+3\chi^{(3)}_{xxyy}\rvert$ for diamond, relative to $\lvert\chi^{(3)}_{xxxx}\rvert$ in LiF is shown in Table II.

The measurement in each of these materials entails somewhat different problems. Diamond is, of course, transparent at both the fundamental and third-harmonic frequency. It is, strictly speaking, an insulator rather than a semiconductor. Its nonlinear susceptibility was measured in transmission relative to LiF, and the result is included here for comparison of the magnitude of the nonlinearity with that of Si and Ge. The clear optical quality diamond available was 0.9 mm thick, and had faces about 7° from the [111] direction. The crystal was oriented so that the E field was parallel to the $[1\bar{1}0]$ direction. There was a wedge angle of 1.2° between the faces. Since the coherence length $l_{\mathrm{coh}}=3.61$ μm is quite short, the transmitted TH signal is given by Eq. (10) with the $\sin^2(\pi z/l_{\mathrm{coh}})$ factor replaced by its average value $\frac{1}{2}$.

Silicon is transparent at the fundamental frequency, but strongly absorbing at the TH. The value for $\lvert\chi^{(3)}_{xxxx}\rvert$ has been determined in transmission, and in reflection with an angle of incidence $\theta_i=20°$. The results for the two independent measurements relative to LiF are in good agreement, and are entered in Table II. The measurement in transmission is more accurate. Since Si is slightly absorbing at 1.06 μm, the [001] cut crystal was 0.06 cm thick. The extinction coefficient was measured to be $(1.0\pm0.1)\times10^{-4}$ cm^{-1} in good agreement with published values.[20]

The dependence of the reflected signal on the angle of incidence θ_i has been published previously for both parallel and perpendicular polarization.[7] The data, which will not be reproduced here, are in excellent agreement with the theoretical behavior described by Eqs. (6) and (6′) displayed in Fig. 3.

Germanium is strongly absorbing at 1.06 μm and thermal damage was observed to occur at much lower power levels than in Si and GaAs. Beam expansion was used as described in Sec. II to avoid damage and still have an observable signal. The reflected TH signal was compared directly to that in Si, and has been converted relative to LiF for incorporation in Table II.

Gallium arsenide presents another problem. Because it lacks a center of inversion, it is capable of strong second-harmonic (SH) generation.[21] Care must be taken to avoid TH generation in a two-step process by sum-frequency generation from SH and the fundamental beams. When the fundamental field is parallel to [001], the SH polarization should vanish. It is important to etch the surface to remove the damaged polished surface layer. The operational criterion for a well-defined crystal symmetry in the SH absorption depth is that the SH signal should have a minimum close to zero.[21] Since the laser beam for TH generation is focused, a small amount of SH signal exists, but it is weak and its beat with the laser beam would yield a TH polarization in the plane of incidence which was

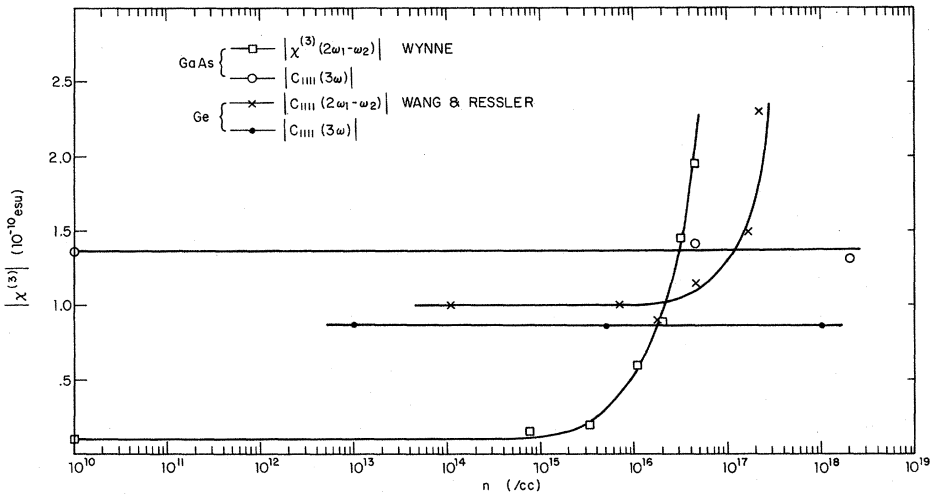

FIG. 6. The nonlinear susceptibility $\chi^{(3)}$ as a function of conduction-electron concentration. Open circle: THG at 0.353 μm in GaAs; open rectangle: frequency mixing near 10 μm in GaAs, from Wynne (Ref. 23); dot: THG at 0.353 μm in Ge; cross: frequency mixing near 10 μm in Ge, from Wang and Ressler (Ref. 24).

eliminated by an additional analyzer at the exit window. Since GaAs is transparent at 1.06 μm, the effect of a fundamental wave reflected from the back surface was eliminated by cutting the sample as a 2.5° wedge. The value of $|\chi^{(3)}_{xxxx}|$ in GaAs relative to Si was measured and is converted relative to LiF in Table II.

A. Effect of Conduction Electrons

All results quoted in Table II were taken with samples of high-resistivity and low-conduction-electron concentration. Data on doped Si, Ge, and GaAs samples with up to $10^{18}/\text{cm}^{-3}$ conduction electrons show no observable contribution of the carriers to $\chi^{(3)}(3\omega)$ for the TH conversion at 3530 Å. This behavior should be contrasted with the strong contribution of conduction electrons to $\chi^{(3)}(2\omega_1-\omega_2)$ for frequency mixing in the infrared, where ω_1 and ω_2 corresponds to 10.6- and 9.6-μ radiation, respectively, from a CO_2 laser. In the latter case the nonparabolicity of the band gives a strong contribution[22,23] in GaAs. A similar, but weaker, contribution has also been observed in Ge.[24] The different results for $\chi^{(3)}$ around the visible region of spectrum and the far infrared are clearly displayed in Fig. 6. This behavior of the conduction-electron contribution is in agreement with the theory of Jha and Bloembergen.[25] Their Eq. (3.16) predicts a negligible contribution from intraband conduction-electron transitions at optical frequencies. At frequencies larger than the band gap, the contribution per conduction electron should be of the same order of magnitude as per valence electron, as shown by Eqs. (2.13)–(2.18) of their paper.[25] Interband contributions dominate the behavior of the susceptibilities. Details of the band structure are less important, but large scale average features such as combined densities of states play an important role. It should be noted that Fig. 6 shows a sizable dispersion in $\chi^{(3)}$ between the infrared and the ultraviolet. While Wynne[23] found that near 10 μm $\chi^{(3)}$ for Ge is about twenty times larger than for Si, the data in Table II show that for TH generation from 1.06 μm $\chi^{(3)}$ for Ge is five times smaller than for Si. It would be of considerable interest to obtain further data on the dispersion of $\chi^{(3)}$ at frequencies large compared to the band gap. A limited amount of data on the dispersion of $\chi^{(2)}$ for SHG in III-V compounds is available.[26,27] Recently theoretical interest in these questions has increased.[28–32]

It has been conjectured that the energy dependence of the collision time of conduction electrons might make an important contribution to $\chi^{(3)}$. We wish to emphasize that such a mechanism cannot be operative at optical THG, where the physical duration of a collision contains many periods of the electromagnetive (EM) oscillations. Whatever its influence may be at an infrared beat frequency $\omega_1-\omega_2$, it certainly should make a negligible contribution at optical frequencies. This point of view has been adopted elsewhere.[33] It is confirmed by our data for high-conductivity semiconductors and metals.

B. Effect of Surface Condition

The results in Table II indicate the preparation of the surface. The mechanical polishing leaves the crystal surface with a damaged layer with a depth on the order of the size of the particles used in the last polishing operation. Within this damaged layer the crystal structure is assumed to be randomly disoriented. The polished surface may also be contaminated by the polishing agent as was found for some of the metals. For Si, which is polished with $\frac{1}{4}$-μ diamond particles, the absorption depth for TH is only 100 Å so that the entire process takes place in the damaged layer. This is also

true for Ge. However, except for anisotropy effects, the THG process does not depend on good crystal structure.

Si and Ge were chemically etched to remove this damaged layer. The reflected TH intensity increased by 20% in Si and by a factor of ~3.5 in Ge. The result for Ge is quite surprising and not completely understood. The question arises as to which result is more characteristic of the intrinsic susceptibility and which is more influenced by spurious effects. One thing to note is that the absolute intensity increase is twice as large in Si as in Ge since the signal from polished Ge is only 3% of the signal from polished Si. Then the increased intensity due to etching could be due to spurious effects of roughly the same magnitude.

Mechanically polished surfaces are often contaminated with the polishing particles, $\frac{1}{4}$-μ diamond and 0.1-μ alumina for Si and Ge samples, respectively. TH generated in these particles can interfere with the reflected signal from the semiconductor. However, in the case of Al, it was observed that the effect of alumina contamination was to increase the reflected THG, the opposite of what is observed here.

It is known that etching causes the growth of an oxide film, which can be contaminated with the etchant.[34] These films cause a characteristically cloudy surface and were sometimes observed on the etched crystals. The films tend to reduce the reflectivity of the surface,[35] increasing the fundamental field in the semiconductor and the reflected THG. There is also some evidence that the effect of a surface film on reflectivity is larger for materials with high absorption,[34] such as Ge. To increase the reflected TH in Si by 20%, the reflectivity has to drop from 36 to 32.2%. The field in Ge would have to increase by 50% to account for $3\frac{1}{2}$ times as much reflected THG. An estimate for Si indicates a 100-Å SiO_2 film would drop the reflectivity by only 0.6% at 5460 Å.[36] So this mechanism seems unlikely to produce the full observed effect. A second mechanism is that any TH generated in the oxide film in transmission would be reflected off the semiconductor and observed as reflected TH. However, the coherence length for these films should be on the order of 1 μ so the generation in an ~100 Å film will be small. If the film is contaminated to the extent that it is somewhat absorbing, the generation could be higher. The anisotropy variation due to destruction of the crystallographic orientation in the polished layer is unable to account for the observed variations.

It appears probable that etching the semiconductors provided good crystalline structure but not a chemically clean surface. It is not clear that etching provided better information about the intrinsic susceptibility of the semiconductors. It would have been better to have used a cleaved surface, which can be made clean and damage free.[36] Except for GaAs, the susceptibility ratios given are for the polished surfaces, which can be made more reproducibly.

V. CIRCULARLY POLARIZED THG AND THE ANISOTROPY OF $\chi^{(3)}$

The general symmetry considerations, referred to in Sec. II, predict that a circularly polarized laser beam cannot produce TH radiation in an isotropic material, nor if the light beam is propagating along a threefold or sixfold axis of symmetry. When propagating along a fourfold axis of symmetry the TH radiation should be circularly polarized in the opposite sense. Macroscopic symmetry arguments predict that these statements should be equally valid for transparent and absorbing media.

We have verified these predictions for the first time in an absorbing glass As_2S_3 and in absorbing cubic crystals Si and GaAs. It is difficult to apply the method of circular polarization in reflection, because deviations causing a slight eccentricity of polarization cannot be avoided on refraction, unless the incidence is exactly normal. We have therefore done experiments with normal incidence in transmission on samples, which are nearly transparent at the fundamental frequency but strongly absorbing at the TH. First the deviation from perfect circularity of the laser pulses was tested by observing the TH signal in a transparent glass. This gives an upper limit for the quantity δ^2 in Eq. (17). The data in Table III show that the TH signal generated by a nominally circularly polarized laser is less than 1% of that generated by a linearly polarized laser beam in the transparent glass.

The same small *ratio* occurs in a As_2S_3 glass which strongly absorbs the TH radiation. Similarly, a circularly polarized light beam propagating along [111] in a Si crystal produces no TH generation, but a strong TH signal is observed when the circularly polarized light propagates along the [100] direction in Si.

The latter process can be understood on an atomistic basis in nonabsorbing media as shown in Fig. 7. In an elementary nonlinear harmonic process, three left circularly polarized quanta are taken from the laser field while a right circularly

TABLE III. TH signal excited by a circularly polarized laser beam relative to that excited by a linearly polarized beam.

Glass slide (transparent)	0.011 ± 0.004
As_2S_3 glass	0.0078 ± 0.003
Si [111] (etched)	0.013 ± 0.005

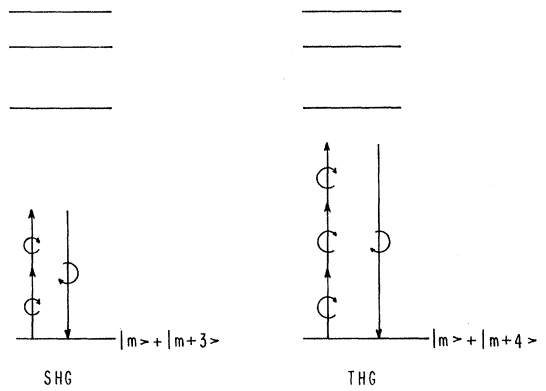

FIG. 7. SHG and THG by circularly polarized light in transparent media. For SHG the electronic ground state must be a superposition of states with $\Delta m = \pm 3$, as provided by a trigonal crystal field potential. For THG the electronic ground state must be a superposition of states with $\Delta m = \pm 4$, as provided by a tetragonal crystal field potential.

polarized quantum is added to the third-harmonic wave. The electronic wave function of the crystal must return through the virtual transitions to the original ground state. Consequently this ground state must be a superposition of wave functions differing by $\Delta m = \pm 4$ in spatial quantum number. It is precisely a crystalline field potential of tetragonal symmetry which provides this admixture. In the elementary scattering process the angular momentum of the electromagnetic field changes by $\pm 4\hbar$, and this angular momentum around the tetragonal axis is taken up by the lattice through the crystalline potential. Around a threefold axis of symmetry only states with $\Delta m = \pm 3$ are admixed. The THG by circularly polarized light cannot take place, but in this case SHG is possible.[10]

The atomistic argument in an absorbing medium is illustrated in Fig. 8. The imaginary part of $\chi^{(3)}(-3\omega, \omega, \omega, \omega)$ occurs as an interference between single- and multiple-photon transitions between the same ground state and the same final state. In general, $\chi^{(3)}$ has an imaginary part when these two energy levels are spaced by $\hbar\omega$, $2\hbar\omega$, or $3\hbar\omega$. In each case the interference will take place for circularly polarized quanta of fundamental and TH field only if the final state and/or the ground state are superpositions of states with spatial quantum numbers differing by $\Delta m = \pm 4$. Thus an atomistic picture also leads to the result that the same selection rules for harmonic generation by circularly polarized laser beams apply equally in absorbing and in transparent media, in agreement with our experimental results.

Since circularly polarized light does not produce THG in isotropic media but does so in cubic crystals, if propagating along an [001] axis, this may serve as a useful method to detect the cubic anisotropy in $\chi^{(3)}$. The anisotropy ratio $3\chi^{(3)}_{xxyy}/\chi^{(3)}_{xxxx}$ may be determined from Eq. (17). Alternatively, the cubic anisotropy $3\chi^{(3)}_{xxyy}/\chi^{(3)}_{xxxx}$ may be determined, with the use of Eq. (16), by means of linearly polarized light with the electric field vector parallel to a cubic axis and a face diagonal of the cubic crystal, respectively. The two experiments determine, respectively, the quantities $|1 - 3\chi^{(3)}_{xxyy}/\chi^{(3)}_{xxxx}|$ and $|1 + 3\chi^{(3)}_{xxyy}/\chi^{(3)}_{xxxx}|$. For nonabsorbing materials the ratio $3\chi^{(3)}_{xxyy}/\chi^{(3)}_{xxxx}$ is real. The two methods should give compatible results and eliminate a possible ambiguity in sign of the anisotropy ratio. The circular polarization method has been applied to a number of alkali halide crystals, for which the anisotropy had previously been determined by mixing of ruby laser light with a Raman Stokes-shifted component generated in benzene. Table IV shows that our new results are consistent with each other and with the earlier data. It could indeed be expected that for the transparent alkali halide crystals the dispersion in the anisotropy between 1.06 and 0.353 μm is negligible.

For absorbing media, the method of circularly polarized light has been applied to Si and GaAs. THG is observed in transmission with the beam propagating along the [001] axis. The result is compared with the TH signal induced by a linear polarization in the [100] direction. This experiment for Si yields with Eq. (17) the value $|1 - 3\chi^{(3)}_{xxyy}/\chi^{(3)}_{xxxx}| = 0.52 \pm 0.07$. In absorbing media the anisotropy ratio is, in general, a complex quantity. Comparing the signal induced by linearly polarized light in the [100] and the [1$\bar{1}$0] directions yields $|1 + 3\chi^{(3)}_{xxyy}/\chi^{(3)}_{xxxx}| = 2.19 \pm 0.14$. Solving these two equations for the complex ratio yields $3\chi^{(3)}_{x,yy}/\chi^{(3)}_{xxxx} = (1.24 \pm 0.14)\exp i(24° \pm 8°)$. This complex anisotropy should be compared with the real anisot-

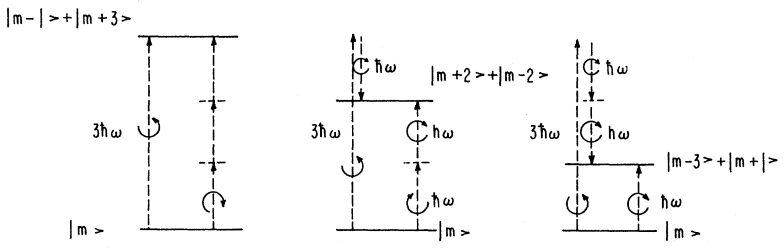

FIG. 8. THG by circularly polarized light in absorbing media. The imaginary part of $\chi^{(3)}$ is caused by an interference of the multiphoton processes shown. This interference requires the admixture of states with $\Delta m = \pm 4$, as occurs in a crystalline field potential of tetragonal symmetry.

TABLE IV. The cubic anisotropy of $\chi^{(3)}$ in alkali halides.

Substance	$1-3\chi^{(3)}_{xxyy}/\chi^{(3)}_{xxxx}$ from Eq. (17)	$1+3\chi^{(3)}_{xxyy}/\chi^{(3)}_{xxxx}$ from Eq. (16)	$3\chi^{(3)}_{xxyy}/\chi^{(3)}_{xxxx}$ our data[a]	$3\chi^{(3)}_{xxyy}/\chi^{(3)}_{xxxx}$ other data[b]
LiF	-0.36 ± 0.08	2.16 ± 0.14	1.36	1.36 ± 0.12
CaF_2	-0.52 ± 0.07	2.48 ± 0.10	1.52	1.52
KCl	$+0.16\pm0.08$	1.94 ± 0.07	0.84	0.91
NaCl	-0.24 ± 0.06	2.24 ± 0.07	1.24	1.30
KBr	-0.10 ± 0.06	2.05 ± 0.07	1.10	1.10

[a]THG from 1.06-μm radiation, deduced from preceding columns.

[b]Frequency mixing results at $2\omega_1-\omega_2$, where ω_1 is the ruby laser frequency and ω_2 is the Stokes-shifted Raman line, which may be polarized parallel or perpendicular to the laser polarization, respectively, according to Ref. 2.

ropy ratio for Si, $3\chi^{(3)}_{xxyy}/\chi^{(3)}_{xxxx}=1.44\pm0.09$, obtained[23] by frequency mixing near 10.6 μm. There is clearly a dispersion of anisotropy in going from the transparent infrared to the absorbing uv region.

In GaAs only the value $|1-3\chi^{(3)}_{xxyy}/\chi^{(3)}_{xxxx}|=0.62\pm0.08$ could be determined. There is no SHG in this geometry, but for a linear polarization in the $[1\bar{1}0]$ direction required to determine $|1+3\chi^{(3)}_{xxyy}/\chi^{(3)}_{xxxx}|$ from Eq. (16) too much SHG would take place. The anisotropy from frequency mixing near 10.6 μm was $1-3\chi^{(3)}_{xxyy}/\chi^{(3)}_{xxxx}=0.85\pm0.02$. Again some dispersion of the cubic anisotropy is present.

VI. THG IN METALS

Reflected THG was investigated in polycrystalline samples of six metals: Be, Mg, Al, Cu, Ag, and Au. In the first two no TH signal was observable. This places an upper limit on the effective value of $|\chi^{(3)}_{av}|$ in these materials. Observable signals were obtained from the other metals. The reflected TH intensity is, however, much smaller than for Si. In Table V we list the observed TH intensity ratios and the derived value for $|\chi^{(3)}_{av}|$ for polycrystalline polished solid metal surfaces, in the case of polarization perpendicular to the plane of incidence at an angle $\theta_i=20°$. If the TH polarization induced by linearly polarized fundamental field is averaged over all crystallite orientations, one obtains for the metals of cubic symmetry

$$\langle\vec{P}^{NL}(3\omega)\rangle_{av}=\chi^{(3)}_{av}E^2\vec{E}=\tfrac{3}{5}(\chi^{(3)}_{xxxx}+2\chi^{(3)}_{xxyy})E^2\vec{E}\,.$$

This quantity is shown in the last column of Table V. The spatial averaging would yield a more complicated expression for the hexagonal metals Be and Mg, but here only an upper limit for $|\chi^{(3)}_{av}|$ can be given. The value of $|\chi^{(3)}_{av}|$ is, of course, derived with the aid of Eqs. (6) and (15), where the value of $F^R_\perp(\theta_i=20°,\epsilon)$ is computed with the aid of the linear optical data given in Table I. It should be noted that $|\chi^{(3)}|$ is quite similar for Cu, Ag, and Au, but an order of magnitude smaller than for Si.

It was found that the data on polished solid samples are less reliable than the data from vacuum deposited films. In fact, it was impossible to obtain reproducible data from polished aluminum.

It is suspected that when the Al was polished with alumina powder, the 0.3-μm Al_2O_3 particles became imbedded in the surface. TH was generated in these particles in transmission and then reflected off the Al surface, completely masking the reflected THG from the Al. Since Al is extremely reactive, evaporated Al typically forms an Al_2O_3 layer of 10–20-Å thickness on its surface. However, a layer this thin should generate negligible TH compared to an effective layer of 0.3 μm. For these reasons the evaporated film results are the most reliable.

When Au was polished with red rouge, it gave four times more reflected signal than an Au evaporated film. When polished with alumina powder, it gave reasonable agreement with the film. Yet when Cu was polished with red rouge, it gave reasonable agreement with a Cu film. Apparently different metals retain the polishing particles to a different degree. In each case the angular dependence of the reflected signal was checked at at least two angles to verify the signal as TH. Also the diffuse reflection was monitored to make sure there was no fluorescence, which sometimes occurred with contaminated surfaces.

In Table VI the data obtained with evaporated films are listed. Note that the TH signal in Al is measured with the polarization parallel to the plane

TABLE V. Experimental reflected intensity ratios and calculated susceptibility ratios for polished metal surfaces.

$F^R_\perp(20°,\epsilon)$	$\frac{I^R_{2\omega}(20°)}{I\text{ (Silicon)}}$	$\frac{\lvert\chi^{(3)}_{av}\rvert}{\lvert\chi^{(3)}_{xxxx}\rvert}$ (Silicon)
Be $8.42^{18.1}_{4.14}\times10^{-4}$	≤0.0008	≤0.014
Mg $2.48^{6.51}_{1.03}\times10^{-4}$	≤0.0009	≤0.026
Cu $2.16^{3.84}_{1.25}\times10^{-4}$	0.0058 ± 0.0011	0.071 ± 0.04
Ag $1.82^{2.20}_{1.51}\times10^{-4}$	0.0087 ± 0.0013	0.094 ± 0.03
Au $1.57^{2.59}_{0.97}\times10^{-4}$	0.0064 ± 0.0008	0.087 ± 0.03

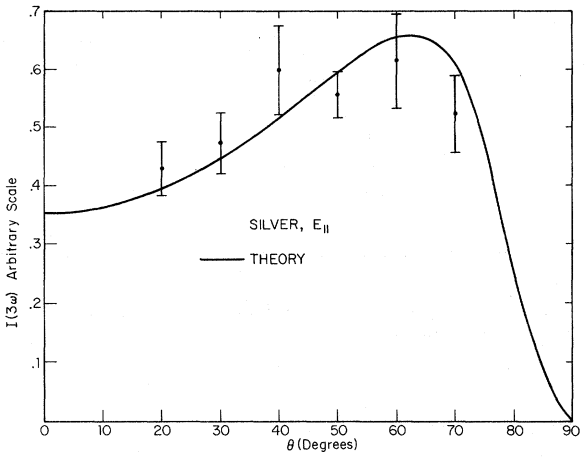

FIG. 9. The angular dependence of THG in silver, with the polarization in the plane of incidence.

of incidence with $\theta_i = 70°$. The reason for this geometry is that it maximizes the quite weak THG from Al. This weakness in the case of Al arises not from a small value of $|\chi^{(3)}_{av}|$. In fact the nonlinear susceptibility is comparable to that of Si and an order of magnitude larger than for the other metals. The small THG in Al is caused by very small values of the $F^R(\theta_i, \epsilon)$ factor in this metal for the frequencies employed. It is seen from Fig. 2 that the complex index of refraction is very high near 1.06 μm. The reflectivity is close to unity and the Fresnel factor is small.

The angular dependence of THG has been observed in Al and Ag for the parallel polarization case. The data are shown in Figs. 9 and 10. The observations are in good agreement with the angular dependence predicted by Eq. (6′). The maximum of the signal for $\theta_i \approx 70°$ in Al is striking.

The relatively larger value of $\chi^{(3)}$ for Al compared to the other metals is related to the strong interband transition near 0.8 μm shown in Fig. 2 close to the fundamental frequency at 1.06 μm. This

TABLE VI. Experimental reflected intensity ratios and calculated susceptibility ratios for evaporated metal films.

	$F^R(\theta, \epsilon)$	$\frac{I_3^R(\theta)}{I\ (\text{Silicon})}$	$\frac{\lvert\chi^{(3)}_{av}\rvert}{\lvert\chi^{(3)}_{xxxx}\rvert\ (\text{Silicon})}$
Al ($\theta = 70°$, ∥ pol.)	$1.12^{1.72}_{0.75} \times 10^{-5}$	0.034 ±0.007	0.68 ±0.35
Cu ($\theta = 20°$, ⊥ pol.)	$2.16^{3.84}_{1.25} \times 10^{-4}$	0.0077 ± 0.011	0.081 ± 0.04
Ag ($\theta = 20°$, ⊥ pol.)	$1.82^{2.20}_{1.51} \times 10^{-4}$	0.0055 ± 0.007	0.075 ± 0.030
Au ($\theta = 20°$, ⊥ pol.)	$1.57^{2.59}_{0.97} \times 10^{-4}$	0.0078 ± 0.010	0.086 ± 0.030

TABLE VII. Susceptibility ratios calculated by Miller's rule extended to THG compared to experimental ratios for metals and semiconductors.

	$\left\lvert\frac{\chi^{(3)}}{\chi^{(3)}_{Al}}\right\rvert_{calc}$	$\left\lvert\frac{\chi^{(3)}}{\chi^{(3)}_{Al}}\right\rvert_{expt}$	$\left\lvert\frac{\chi^{(3)}}{\chi^{(3)}_{Si}}\right\rvert_{calc}$	$\left\lvert\frac{\chi^{(3)}}{\chi^{(3)}_{Si}}\right\rvert_{expt}$
Be	0.003	≤0.021		
Mg	0.016	≤0.038		
Al	1	1	270	0.68
Cu	0.018	0.12		
Ag	0.026	0.11		
Au	0.023	0.14		
Si			1	1
Ge			2.1	0.22
GaAs			0.31	0.54
LiF			1.20×10^{-5}	1.17×10^{-5}
Diamond			9.0×10^{-3}	0.62×10^{-3}

same resonance makes the F factor for this metal anomalously small at the frequencies of interest in our experiment. The small values of $|\chi^{(3)}_{av}|$ for Be and Mg may be correlated with smaller values for the linear dielectric constants. These metals also have very nearly filled bands.

In Table VII an attempt is made to make this correlation more quantitative by using a modified Miller-type relationship for $\chi^{(3)}$, as was previously employed by Wynne.[23] Such a relationship can only be expected to have a qualitative significance in

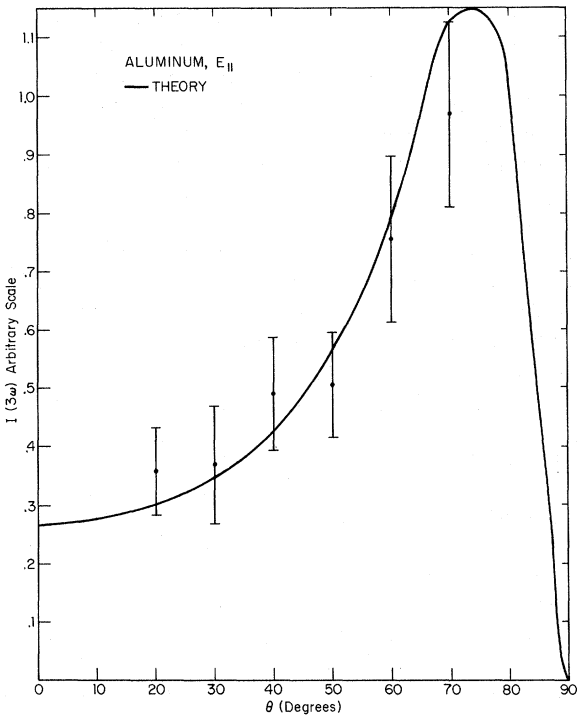

FIG. 10. The angular dependence of THG in aluminum, with the polarization in the plane of incidence.

strongly dispersive regions of the nonlinearity. Table VII shows that there is not a good correlation. This becomes even more evident if we attempt to make a correlation relative to the semiconductors and insulators also listed in Table VII. The variance between the experimental and computed ratios in the homologous series C, Si, and Ge is pronounced, but an order-of-magnitude trend is indeed present. The nonlinear susceptibility can be expected to be larger in materials with the larger linear susceptibility. Extensions of the theory[28-32] are necessary to obtain estimates for $\chi^{(3)}$ in absorbing solids.

VII. CONCLUSION

By means of picosecond pulse trains from mode-locked lasers THG and related third-order nonlinear susceptibilities can be observed in strongly absorbing materials. The dispersion characteristics of $\chi^{(3)}$ can and should be measured over a wide frequency range. The theory of this dispersive behavior should also be refined. Circularly polarized beams are useful in determining the cubic anisotropy of $\chi^{(3)}$, both in transparent and absorbing media.

ACKNOWLEDGMENTS

The authors gratefully acknowledge the assistance of and critical discussions with Dr. M. Matsuoka in the early phases of this work. The assistance of S. Mauriei in sample preparation is also acknowledged.

---

*Research supported by the Joint Services Electronics Program under Contract No. N00014-67-A-0298-0006.

A more detailed description of this work may be found in W. K. Burns, Ph.D. thesis (Harvard University, 1971) (unpublished).

†Present address: Arthur D. Little Inc., Cambridge, Mass.

[1]R. W. Terhune, P. D. Maker, and C. M. Savage, Phys. Rev. Letters 8, 404 (1962); in *Proceedings of the Third International Conference on Quantum Electronics*, edited by P. Grivet and N. Bloembergen (Dunod, Paris, 1963), p. 1559.

[2]P. D. Maker and R. W. Terhune, Phys. Rev. 137, A801 (1965).

[3]G. H. C. New and J. F. Ward, Phys. Rev. Letters 19, 556 (1967); J. F. Ward and G. H. C. New, Phys. Rev. 185, 57 (1969).

[4]P. P. Bey, J. F. Giuliani, and H. Rabin, Phys. Rev. Letters 19, 819 (1967); see also R. K. Chang and L. K. Galbraith, Phys. Rev. 171, 993 (1968).

[5]P. P. Bey, J. F. Giuliani, and H. Rabin, Phys. Letters 28A, 89 (1968).

[6]Charles C. Wang and E. L. Baardsen, Phys. Rev. 185, 1079 (1969); Phys. Rev. B 1, 2827 (1970).

[7]N. Bloembergen, W. K. Burns, and M. Matsuoka, Opt. Commun. 1, 195 (1969).

[8]P. P. Bey and H. Rabin, Phys. Rev. 162, 794 (1967).

[9]P. P. Bey, J. F. Giuliani, and H. Rabin, Phys. Letters 26A, 128 (1968).

[10]H. J. Simon and N. Bloembergen, Phys. Rev. 171, 1104 (1968).

[11]C. L. Tang and H. Rabin, Phys. Rev. B 3, 4025 (1971).

[12]N. Bloembergen, in *Polarization Matière et Rayonnement*, edited by Société Francaise de Physique (Presses Universitaires de France, Paris, 1969), p. 109; see also N. Bloembergen, *Physics of the Solid State*, edited by S. Balakrishna *et al.* (Academic, New York, 1970), Chap. 15.

[13]N. Bloembergen, W. K. Burns, and C. L. Tang, Intern. J. Quantum Chem. (to be published).

[14]J. A. Armstrong, N. Bloembergen, J. Ducuing, and P. S. Pershan, Phys. Rev. 127, 1918 (1962).

[15]N. Bloembergen and P. S. Pershan, Phys. Rev. 128, 606 (1962).

[16]N. Bloembergen, Opt. Acta 13, 311 (1966), and references quoted therein.

[17]A. J. DeMaria, W. H. Glenn, Jr., M. J. Brienza, and M. E. Mack, Proc. IEEE 57, 2 (1969), and references contained therein.

[18]G. Hass, J. Opt. Soc. Am. 45, 945 (1955).

[19]H. C. Gatos and M. C. Lavine, MIT Lincoln Laboratory Technical Report No. 293, 1963 (unpublished).

[20]G. G. Macfarlane and V. Roberts, Phys. Rev. 98, 1865 (1955).

[21]R. K. Chang and N. Bloembergen, Phys. Rev. 144, 775 (1966).

[22]C. K. N. Patel, R. F. Slusher, and P. A. Fleury, Phys. Rev. Letters 17, 1011 (1966).

[23]J. J. Wynne, Phys. Rev. 178, 1295 (1969); J. J. Wynne and G. D. Boyd, Appl. Phys. Letters 12, 191 (1968).

[24]C. C. Wang and N. W. Ressler, Phys. Rev. 188, 1291 (1969).

[25]S. S. Jha and N. Bloembergen, Phys. Rev. 171, 891 (1968); J. Quantum Electron. QE-4, 670 (1968).

[26]R. K. Chang, J. Ducuing, and N. Bloembergen, Phys. Rev. Letters 15, 415 (1965).

[27]F. G. Parsons and R. K. Chang, Opt. Commun. 3, 173 (1971).

[28]Chr. Flytzanis, Phys. Letters 31A, 273 (1970), and references quoted therein.

[29]B. F. Levine, Phys. Rev. Letters 22, 787 (1969); 25, 440 (1970).

[30]J. A. Van Vechten and D. E. Aspnes, Phys. Letters 30A, 346 (1969).

[31]J. A. Van Vechten, M. Cardona, D. E. Aspnes, and R. M. Martin, Proceedings of the Tenth International Conference on Semiconductors, Cambridge, Mass., 1970 (unpublished).

[32]M. Cardona and F. H. Pollak (unpublished).

[33]N. Bloembergen, private communication as quoted in Ref. 25.

[34]K. Vedam, W. Knausenberger, and F. Lukes, J. Opt. Soc. Am. 59, 64 (1969).

[35]D. K. Burge and H. E. Bennett, J. Opt. Soc. Am. 54, 1428 (1964).

[36]G. W. Gobeli and F. G. Allen, J. Phys. Chem. Solids 14, 23 (1960); Phys. Rev. 127, 149 (1962).